IEEE Access
Multidisciplinary | Rapid Review | Open Access Journal

Received March 3, 2022, accepted March 24, 2022, date of publication March 28, 2022, date of current version April 1, 2022.

Digital Object Identifier 10.1109/ACCESS.2022.3162838

Low-Complexity PSO-Based Resource Allocation Scheme for Cooperative Non-Linear SWIPT-Enabled NOMA

CARLA E. GARCÍA, (Graduate Student Member, IEEE), MARIO R. CAMANA, (Graduate Student Member, IEEE), AND INSOO KOO

Department of Electrical, Electronic and Computer Engineering, University of Ulsan, Ulsan 44610, South Korea

Corresponding author: Insoo Koo (iskoo@ulsan.ac.kr)

This work was supported in part by the National Research Foundation of Korea through the Korean Government Ministry of Science and ICT (MSIT) under Grant NRF-2021R1A2B5B01001721, and in part by the Regional Innovation Strategy (RIS) through the National Research Foundation of Korea (NRF) funded by the Ministry of Education (MOE) under Grant 2021RIS-003.

ABSTRACT Cooperative networks integrating non-orthogonal multiple access (NOMA) and simultaneous wireless information power transfer (SWIPT) are emerging technologies that have been investigated as potential techniques to support the proliferation of the Internet of Things (IoT) and to obtain greener communications. In this sense, the optimization of resource allocation schemes is crucial to improve the performance of future cooperative wireless networks. However, conventional optimization methods that attempt to find the optimal solution may entail high computational complexity. Therefore, we propose a low-complexity particle swarm optimization (PSO)-based scheme to solve the resource allocation problem in a cooperative non-linear SWIPT-enabled NOMA system with a non-linear energy harvesting (EH) user. Specifically, we consider two optimization problems. First, we minimize transmission power, and second, we maximize energy efficiency subject to meeting quality-of-service (QoS) constraints. The problems are non-convex and challenging to solve. Furthermore, we develop the optimal solution based on convex optimization and the exhaustive search (ES) method to validate the results of the proposed PSO-based framework. Afterward, we investigate the performance of five swarm intelligence-based baseline schemes and evaluate an additional low-complexity solution based on the cuckoo search (CS) technique. For comparison purposes, we use orthogonal multiple access (OMA), equal power splitting (EPS), and time fixed (TF) baseline schemes. To our satisfaction, the proposed SWIPT NOMA network outperforms the benchmark schemes, and the proposed PSO-based framework achieves the nearest performance to the optimal scheme with lower complexity than obtained by the comparative swarm intelligence techniques and from convex optimization with the ES method.

INDEX TERMS Cuckoo search, non-linear simultaneous wireless information power transfer, non-orthogonal multiple access, particle swarm optimization, resource allocation.

I. INTRODUCTION

Currently, the limited spectrum and energy resource utilization problem is one of the main concerns for the development of future wireless technologies that permit proliferation of the Internet of Things (IoT), device-to-device (D2D) communications, spectrum sharing, massive machine-type communications, and so on [1]. To enhance spectrum efficiency, non-orthogonal multiple access (NOMA) is an emerging technique enabling multiple users to share the same time–frequency resource block. NOMA can be classified into power and code domains. In this paper, we focus on power-domain NOMA where the transmitter sends all the messages of the users by utilizing different power levels for each user in accordance with their channel conditions, i.e., the messages of users with weaker channel conditions are transmitted with more power than messages of users with stronger channel conditions. At the receiver, users with better channel conditions perform successive interference cancellation (SIC) to remove interference caused by users with stronger channel conditions, and users with the weakest

The associate editor coordinating the review of this manuscript and approving it for publication was Stefano Scanzio.

channel conditions decode messages by treating the other messages as noise [2].

Moreover, efficient energy harvesting (EH) techniques have been investigated to improve energy efficiency in limited-processing-power and low-power energy-constrained communication networks, such as wireless body area networks, IoT devices, and wireless sensor networks [3]–[6]. Particularly with small communication devices, one of the main challenges is to autonomously maintain connectivity and maximize network lifetime. In this regard, the radio frequency (RF) EH technique is capable of receiving RF signals and converting them to electricity to extend the battery lifetime of communications devices and avoid wasted power [7]. Indeed, through the application of EH technology, conventional batteries can be eliminated, which entails cost reductions, eliminating wires, and promoting environmentally friendly technologies [8]. One main application of the RF-EH technique is simultaneous wireless information and power transfer (SWIPT). SWIPT technology allows users to receive information and harvest energy from the received RF signal at the same time [9]. SWIPT appears to be a powerful technique, providing energy-efficient green communications, especially in emergency situations. For instance, in [10], SWIPT was integrated into a device-to-device (D2D) system to assist natural disaster communications where replacing or recharging batteries is a critical issue.

Among the benefits of SWIPT is prolonging the lifetime of energy-constrained networks since SWIPT users can serve as cooperative relays to edge nodes. Furthermore, SWIPT-enabled NOMA systems have demonstrated meaningful yields over the conventional orthogonal multiple access (OMA) scheme in terms of spectral efficiency [11], energy efficiency [11]–[13], power consumption [7], [14], [15], and secrecy sum rate [16]. For instance, the authors in [11], [12], and [17] maximized energy efficiency in NOMA SWIPT systems subject to the quality of service (QoS) by utilizing analytical approaches. The results showed that SWIPT-enabled NOMA systems satisfactorily outperformed the conventional OMA. Moreover, energy-saving designs are crucial to establishing eco-friendly communication systems. Therefore, optimization problems have been addressed to minimize the power in wireless networks [7], [15]. In this sense, Luo *et al.* [7] designed a deep learning scheme to find an approximately optimal solution for minimizing total transmission power in a SWIPT NOMA network. Garcia *et al.* derived a closed-form solution to minimize the total transmission power of a cooperative system aided by a collaborative SWIPT user [15]. The outcomes of these studies verified the superiority of NOMA over baseline multiple access schemes. It is worth noting that not one of the previous articles considered non-linear EH, which greatly increases the difficulty in solving the optimization problem due to coupled variables involved in problem resolution.

To suitably design a SWIPT system, a fundamental requirement is to accurately model the EH circuit that allows transforming the received RF signal into a direct current (DC) signal. Although the employment of linear EH models still prevails in most of the literature, recent investigations have highlighted the importance of including realistic models of EH circuits in the analysis of communications systems [18], [19]. Indeed, practical EH reveals a non-linear relation between the stored energy and the received RF power because of physical impairments, such as non-ideal energy conversion efficiency, storage imperfections, non-linear circuits, etc. [20], [21]. Consequently, to leverage the advantages of SWIPT and acquire more-accurate results, the application of realistic EH models must be integrated into wireless SWIPT systems.

Although nonlinear EH models consider a more realistic environment, reluctance to adopt them still exists because of the complexity in solving the optimization problems. Conventional optimization methods attempting to find the optimal solution may entail high computational complexity, and a closed-form solution is inflexible to change since it needs to be reformulated after a change in the network [15]. Therefore, the metaheuristic branch of artificial intelligence (AI) algorithms has opened doors to dealing with complex computational problems. Metaheuristics generate possible solutions to optimization problems and select the best one with low complexity and high accuracy. Overall, the most popular metaheuristic algorithms in the fields of science and engineering include the genetic algorithm [22], the cuckoo search (CS) [23], and particle swarm optimization (PSO) [24]. For instance, Mohiz *et al.* [23] discussed different metaheuristic algorithms and identified which ones work the best to optimize the placement of tasks for network-on-chip cores. The paper concluded that CS is more suitable for placement with a low computational overhead. Moreover, hybrid schemes have been developed by combining two or more characteristics of the original metaheuristic algorithms to enhance optimization results [25].

Motivated by the advantages provided by metaheuristic algorithms for solving complex optimization problems, this paper investigates the application of swarm intelligence schemes for solving resource allocation optimization problems in a nonlinear SWIPT NOMA green communication system. Among them, we propose the PSO-based scheme as a potential solution that achieves high accuracy with low complexity. To evaluate the performance of the proposed network even further, we formulated two different optimization problems: power transmission minimization and energy efficiency maximization. The main contributions of this paper can be summarized as follows.

- The goal is to optimize total transmission power and energy efficiency in a cooperative, non-linear, SWIPT-enabled NOMA system with a non-linear EH user while satisfying the constraints on minimum data rates, minimum harvested energy at the terminal, time fraction, and power splitting ratio range.
- The optimization problems considered are non-convex involving joint optimization of the time transmission

fraction, power-splitting ratio, and power allocation and are thus difficult to solve directly. To tackle this issue, we propose a low-computational-complexity scheme based on PSO. Moreover, we compare the performance of five swarm intelligence-based baseline schemes and develop a low-complexity solution based on CS [26]–[28]. To validate the performance of the proposed PSO scheme, we provide an analytical approach based on convex optimization with the exhaustive search (ES) method, denoted as CVX+ES.

- Furthermore, we analyze the effect from linearity of EH on the transmit power and energy efficiency of the proposed scheme (SWIPT NOMA cooperative communication optimizing the power variables, time factor, and the power-splitting ratio) and the following baseline schemes: SWIPT NOMA cooperative communication with a time fixed (TF) scheme, and SWIPT NOMA cooperative communication with equal power splitting (EPS). Moreover, we investigate the conventional OMA baseline scheme for comparison purposes. To our satisfaction, simulation results demonstrated that the proposed cooperative non-linear SWIPT-NOMA system reduces more transmission power and can obtain higher energy efficiency than the benchmark schemes.
- Numerical results show that the outcomes obtained by PSO reach near-optimal performance, compared to those obtained by optimal (but time- and energy-consuming) convex optimization with the ES method [27]. In addition, we provide a complexity comparison between the optimal scheme (CVX+ES) and the swarm intelligence schemes in terms of computation time. Thus, we validated PSO as achieving convergence faster than the CS-based framework and with less computational time.

The rest of the paper is organized as follows. The system model is described in Section II. In Section III, we formulate the optimization problems of total transmission power minimization and energy efficiency maximization, and we present the proposed PSO-based solution and comparison approaches. Finally, numerical results and the conclusion are presented in Section IV and Section V, respectively.

II. SYSTEM MODEL

We propose a cooperative, non-linear, SWIP-enabled NOMA system composed of three users and one transmitter, as shown in Figure 1, where all nodes have one single antenna. Moreover, the user close to the transmitter, denoted by u_2, acts as a cooperative decode-and-forward (DF) relay that provides SWIPT to aid a distant user, u_1, to receive messages. Assume there is no direct transmission link between the transmitter and distant user u_1 because of the shadowing effect and obstacles. User 3 acts as a non-linear RF EH user (denoted by u_3) capable of providing an alternative power supply for electronic devices where conventional energy sources are costly or difficult to implement because of remote locations, areas of catastrophic damage, or toxic environments.

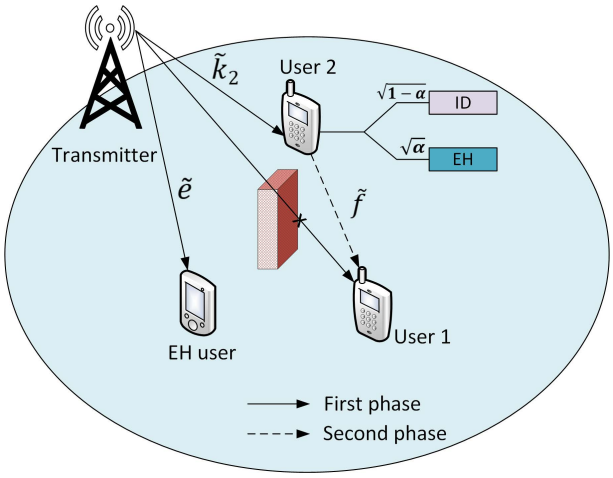

FIGURE 1. Cooperative non-linear SWIPT-enabled NOMA system.

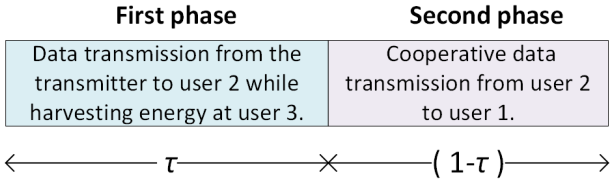

FIGURE 2. Frame structure of the considered cooperative non-linear SWIPT enabled NOMA system.

A transmission is completed in two phases, as shown in Figure 2. In the first phase, the transmitter performs superposition coding according to the NOMA principles by sending the messages of u_1 and u_2 to nearby user u_2, while u_3 extracts RF power by receiving the superimposed signal from the transmitter. In the second phase, u_2 forwards message 1 to u_1 by utilizing the stored energy obtained during the first phase. More details on the first and second phases are in the following subsections.

A. FIRST PHASE

In the first phase, the transmitter conveys a superimposed signal denoted by x, $x = m_1x_1 + m_2x_2$, where $x_1, x_2 \in \mathbb{C}$ are the independent and identically distributed $(i.i.d)$ messages for u_1 and u_2, respectively. Moreover, the transmitted symbol is normalized as $\mathbb{E}\left(|x_1|^2\right) = \mathbb{E}\left(|x_2|^2\right) = 1$, and the power variables are denoted by m_1 and m_2, for u_1 and u_2, respectively. At the receiver, u_2 provides SWIPT by dividing the superimposed received signal into two parts according to power-splitting ratio α, one for information decoding and the other for energy harvesting. Accordingly, the received signal for information decoding at u_2 can be given by

$$y_2^{(1)} = \sqrt{1-\alpha}\tilde{k}_2\left(m_1x_1 + m_2x_2\right) + z_2^{(1)}, \tag{1}$$

where $\tilde{k}_2$ is the channel coefficient between the transmitter and user 2, $z_2^{(1)} \sim \mathcal{CN}\left(0, \sigma_2^2\right)$ is the additive white gaussian noise (AWGN), and $\alpha \in (0, 1)$ is the power-splitting ratio.

In accordance with NOMA principles, since u_2 has the strongest channel conditions, it employs SIC to first decode the message of u_1 and then subtracts this message from the received signal to decode its message, x_2, without interference. Consequently, the signal-to-interference-plus-noise ratio (SINR) of u_2 when decoding message 1, x_1, is described in equation (2), and the signal-to-noise ratio (SNR) of u_2 when decoding its own message, x_2, is equation (3):

$$SINR_{2,x_1}^{(1)} = \frac{(1-\alpha)\, k_2 m_1^2}{(1-\alpha)\, k_2 m_2^2 + \sigma_2^2}, \tag{2}$$

where $k_2 = \left|\widetilde{k_2}\right|^2$,

$$SNR_{2,x_2}^{(1)} = \frac{(1-\alpha)\, k_2 m_2^2}{\sigma_2^2}. \tag{3}$$

Hence, the rate for the distant user's data and the rate for the nearby user's data at u_2 can be given by (4) and (5), respectively:

$$R_{x_1,u_2}^{(1)} = \tau \log_2\left(1 + SINR_{2,x_1}^{(1)}\right), \tag{4}$$

and

$$R_{u_2} = \tau \log_2\left(1 + SNR_{2,x_2}^{(1)}\right), \tag{5}$$

where $\tau \in (0, 1)$ is the transmission time fraction for the first phase.

Furthermore, in the theoretical linear model of an EH circuit, the users harvest all the power of the incoming signal. For instance, the linear model of the energy harvested by u_2 can be written as:

$$Eh_{2\_linear}^{(1)} = \tau \eta \alpha k_2 \left(m_1^2 + m_2^2\right), \tag{6}$$

where η is the energy harvesting efficiency. However, the practical non-linear EH model is given by the logistic function that includes the saturated harvested power and circuit specifications. Therefore, the energy stored by u_2 follows the nonlinear EH model in [9], and can be calculated as follows:

$$Eh_2^{(1)} = \tau \frac{\psi_{u_2} - L\Omega}{1-\Omega}, \tag{7}$$

where $\Omega = \frac{1}{1+\exp(ab)}$ and $\psi_{u_2} = \frac{L}{1+\exp\left(-a\left(p_{int_{u2}} - b\right)\right)}$, in which $p_{int_{u2}}$ denotes the input power. In this case, $p_{int_{u2}} = \alpha k_2 \left(m_1^2 + m_2^2\right)$. L is a constant that sets the maximum harvested power at the EH receiver when the EH circuit is saturated. Parameters a and b are constants depending on the detailed circuit specifications, for example, capacitance, resistance, and diode turn-on voltage. We consider the values adopted in [9], which are $L = 3.9mW$, $a = 1500$, and $b = 0.0022$. For simplicity, we assume the energy stored by user 2 is only utilized for transmitting information to user 1, and energy consumption for signal processing and maintaining the circuit can be ignored [12]. Therefore, the transmit power at user 2 can be given by

$$P_{sw} = \frac{Eh_2^{(1)}}{1-\tau}. \tag{8}$$

Finally, the energy harvested by u_3 utilizes the nonlinear EH model described in [9] and can be expressed by

$$Eh_3^{(1)} = \tau \frac{\psi_{u_3} - L\Omega}{1-\Omega}. \tag{9}$$

Here, $\psi_{u_3} = \frac{L}{1+\exp\left(-a\left(p_{int_{u3}} - b\right)\right)}$, and $p_{int_{u3}} = |\tilde{e}|^2 \left(m_1^2 + m_2^2\right)$, where $\tilde{e}$ is the channel coefficient from the transmitter to user 3. Note that the ideal linear EH model for u_3 can be expressed as

$$Eh_{3\_linear}^{(1)} = \tau \eta |\tilde{e}|^2 \left(m_1^2 + m_2^2\right). \tag{10}$$

B. SECOND PHASE

In this phase, nearby user u_2 utilizes its stored energy to forward message x_1 to u_1. Thus, the received signal at u_1 is

$$y_1^{(2)} = \sqrt{P_{sw}}\widetilde{f} x_1 + z_1^{(2)}, \tag{11}$$

where $\widetilde{f}$ is the channel coefficient from u_2 to u_1, and $z_1^{(2)} \sim \mathcal{CN}\left(0, \sigma_1^2\right)$ is AWGN at u_1. Then, the SNR to decode x_1 is expressed by

$$SNR_{1,x_1}^{(2)} = \frac{P_{sw}\left|\tilde{f}\right|^2}{\sigma_1^2} = \frac{Eh_2^{(1)} \cdot f}{(1-\tau)}, \tag{12}$$

where $f = \frac{\left|\tilde{f}\right|^2}{\sigma_1^2}$. Then, the rate for the distant user's data at u_1 can be written as seen in (13):

$$R_{x_1,u_1}^{(2)} = (1-\tau)\log_2\left(1 + SNR_{1,x_1}^{(2)}\right). \tag{13}$$

III. PROBLEM FORMULATION AND SOLUTION

A. TRANSMISSION POWER OPTIMIZATION PROBLEM

In this problem, we aim to minimize the total transmission power of the cooperative non-linear SWIPT-enabled NOMA system with a nonlinear EH user by jointly optimizing the transmission time fraction, τ, the power-splitting ratio, α, and power allocation variables m_1^2 and m_2^2 while satisfying the QoS constraints from all users. For simplicity, let us define $m_1^2 = p_1$ and $m_2^2 = p_2$. Then, the resource allocation problem to minimize the total transmission power is equivalent to the minimization of $p_1 + p_2$, which can be formulated as follows:

$$\min_{p_1,p_2,\tau,\alpha} p_1 + p_2 \tag{14a}$$

$$\text{s.t. } \tau \log_2\left(1 + \frac{(1-\alpha)\, k_2 p_1}{(1-\alpha)\, k_2 p_2 + \sigma_2^2}\right) \geq \gamma_1, \tag{14b}$$

$$(1-\tau)\log_2\left(1 + f\tau \frac{\psi_{u_2} - L\Omega}{(1-\Omega)(1-\tau)}\right) \geq \gamma_1 \tag{14c}$$

$$\tau \log_2\left(1 + \frac{(1-\alpha)\, k_2 p_2}{\sigma_2^2}\right) \geq \gamma_2, \tag{14d}$$

$$\tau \frac{\psi_{u_3} - L\Omega}{1-\Omega} \geq \phi, \tag{14e}$$

$$p_1 + p_2 \leq P^{\max} \tag{14f}$$

$$0 < \alpha < 1, \tag{14g}$$
$$0 < \tau < 1, \tag{14h}$$

where (14b) and (14c) guarantee that the rate of distant-user data at u_2 and u_1, respectively, can reach the minimum rate requirement constraint, γ_1. Equation (14d) corresponds to the minimum rate constraint for u_2, in which γ_2 denotes the minimum rate target. Equation (14e) corresponds to the minimum harvested power constraint for u_3, in which ϕ denotes the minimum harvested power requirement. Constraint (14f) guarantees that the power to transmit message 1 and message 2 does not exceed the maximum available power at the transmitter. Constraint (14g) indicates that the power splitting ratio, α, is between 0 and 1. Constraint (14h) points out that the time factor, τ, is between 0 and 1.

We can see that this problem is non-convex because of constraints (14b) to (14e). Specifically, (14b) is non-convex due to coupled power allocation variables p_1 and p_2, power-splitting ratio α, and time fraction τ. Moreover, (14c) is non-convex due to the coupled fraction time, τ, and due to ψ_{u_2}, which is challenging because ψ_{u_2} involves the sum of the power allocation variables p_1 and p_2 multiplied by power splitting ratio α. Similarly, constraint (14e) is non-convex due to the coupled fraction time, τ, and ψ_{u_3}. In (14e), ψ_{u_3} involves the sum of the power allocation variables p_1 and p_2. Thus, optimization problem (14) is difficult to solve directly. Conventional optimization techniques and ES methods are used to solve resource allocation problems when searching for the optimal solution. However, these techniques involve high complexity due to a high computational load that entails undesired delays in updating the optimal solution. Moreover, if an additional element is involved in the network, a closed-form solution should be reformulated. Therefore, we investigate low-complexity solutions to solve the proposed resource allocation problems more efficiently with much lower complexity and without degrading the network performance. We particular studied the potential PSO framework to obtain a low-complexity solution in the proposed cooperative non-linear SWIPT-enabled NOMA system. Moreover, we investigated CS and CVX+ES-based frameworks for comparison purposes. In addition, we considered two baseline schemes based on an EPS ratio and a TF scheme.

1) ANALYTICAL SOLUTION FOR TRANSMISSION POWER MINIMIZATION

Since problem (14) is non-convex and cannot be directly solved, let us fix the value of variable τ for any given $\tau \in (0, 1)$ to transform non-convex optimization problem (14). Then, after some derivations, problem (14) is transformed into a convex problem as follows:

$$\min_{p_1,p_2,\alpha} p_1 + p_2 \tag{15a}$$
$$\text{s.t. } \nu_{u1,2} k_2 p_2 + \frac{\nu_{u1,2}\sigma_2^2}{(1-\alpha)} - k_2 p_1 \leq 0, \tag{15b}$$
$$\frac{\kappa_{u2}}{\alpha} - k_2 (p_1 + p_2) \leq 0, \tag{15c}$$
$$\frac{\nu_{u2}\sigma_2^2}{(1-\alpha)} - k_2 p_2 \leq 0, \tag{15d}$$
$$\kappa_{u3} - |\tilde{e}|^2 (p_1 + p_2) \leq 0, \tag{15e}$$
$$p_1 + p_2 \leq P^{\max} \tag{15f}$$
$$0 < \alpha < 1, \tag{15g}$$

where $\nu_{u1,2} = \left(2^{\frac{\gamma_1}{\tau}} - 1\right)$, $\nu_{u2} = \left(2^{\frac{\gamma_2}{\tau}} - 1\right)$, $\kappa_{u3} = b - \frac{1}{a}\ln\left(\frac{L}{L\Omega+(1-\Omega)\frac{\phi}{\tau}} - 1\right)$, $\kappa_{u2} = b - \frac{1}{a}\ln\left(\frac{L}{L\Omega+(1-\Omega)\chi_{u2}} - 1\right)$, $\chi_{u2} = \frac{\nu_{u1,1}(1-\tau)}{f\tau}$, and $\nu_{u1,1} = \left(2^{\frac{\gamma_1}{1-\tau}} - 1\right)$.

Problem (15) is convex and can be solved by the CVX toolbox in MATLAB [34]. The optimal value of τ is obtained with a one-dimensional ES method. For each candidate value of τ, problem (15) needs to be solved to evaluate the objective function. The ES method gives the optimal value of τ but entails high computational complexity. Then, this method can be considered the optimal solution for comparative analysis. In addition, a near-optimal value of τ can be obtained by using metaheuristic methods, such as PSO or CS, to reduce the load computational complexity. Therefore, in Subsection III.A.2 and Subsection III.A.3, we propose PSO and CS-based approaches for transmission power minimization.

2) PROPOSED PSO-BASED FRAMEWORK FOR TRANSMISSION POWER MINIMIZATION

PSO is a potential optimization scheme based on a population called the swarm, which is composed of particles that move together in a search space, with the objective being to find the optimal solution. Each particle contains the variables to be optimized, and its position is updated each iteration towards the local and global best positions. The global best position indicates the position in which a particle has reached the best yield in the population, whereas the local best position indicates the position in which the particle has reached its own best yield so far. In this paper, each particle position is denoted by $\mathbf{q}_r$, which is a vector of four elements (p_1, p_2, α, and τ) that correspond to the set of variables to be optimized, and it can be written as follows:

$$\mathbf{q}_r = \left\{q_{p_1,r}, q_{p_2,r}, q_{\alpha,r}, q_{\tau,r}\right\}, \tag{16}$$

where $r = 1, 2, 3, \ldots, R_p$, in which R_p denotes the number of particles in the swarm. Moreover, the feasible search region for each element of the particle's position, $q_{p_1,r}, q_{p_2,r}$, is denoted as $[0, P^{\max}]$, where $P^{\max}$ is the maximum transmission power at the transmitter. The search region for the particle's position, $q_{\alpha,r}$ and $q_{\tau,r}$, is the range $(0, 1)$.

Since proposed problem (14) is a constrained optimization problem, a method to deal with constraints is required. Therefore, we utilize the penalty method, where fitness function $f(\mathbf{q}_r) = f(p_1, p_2, \alpha, \tau)$ is based on the objective

function of problem (14) as follows:

$$f(\mathbf{q}_r) = p_1 + p_2 + \varsigma \sum_{i=1}^{4} \xi(g_i), \tag{17}$$

where ς is the penalty value, g_i is the i-th constraint of problem (14), and $\xi(g_i) = 0$ if g_i is satisfied, whereas $\xi(g_i) = 1$, otherwise. If all constraints are satisfied, $f(\mathbf{q}_r)$ is the objective function without penalty.

Furthermore, the search strategy to find the optimal solution is based on updating each particle's velocity and position. Based on [15], the velocities of the particles are updated as follows:

$$\mathbf{v}_r^{t+1} = Ine^t \mathbf{v}_r^t + j_1 c_1 \left(\mathbf{lb}_r^t - \mathbf{q}_r^t\right) + j_2 c_2 \left(\mathbf{gb}^t - \mathbf{q}_r^t\right), \tag{18}$$

where Ine^t denotes the inertia weight for the velocity update, v_r^t is the velocity of the r-th particle in the t-th iteration, $\mathbf{lb}_r^t$ denotes the local best position of the r-th particle, $\mathbf{q}_r^t$ denotes the position of the r-th particle in the t-th iteration, and $\mathbf{gb}^t$ denotes the global best position of all particles in the t-th iteration; j_1 and j_2 are random numbers between 0 and 1, and c_1 and c_2 are the cognitive and social parameters, respectively.

Then, to update the r-th particle's position for each of the elements described in (16), the previous particle position plus the updated velocity indicated in (18) are considered as follows:

$$\mathbf{q}_r^{t+1} = \mathbf{q}_r^t + \mathbf{v}_r^{t+1}. \tag{19}$$

The procedure of the proposed PSO-based algorithm in solving the power minimization problem (14) is described in Algorithm 1, where the input parameters correspond to the maximum transmission power at the transmitter, $P^{\max}$; the target rate of user 1, γ_1; the target rate value of user 2, γ_2; the minimum energy harvesting at user 3, ϕ; the maximum number of iterations, denoted by I_{PSO}^{total}; the number of particles, R; the inertia weight for the velocity update, Ine; random numbers j_1, j_2, and cognitive and social parameters c_1 and c_2. Moreover, the initial global best position is allocated in accordance with the objective function, wherein this paper the initial **gb** selects the minimum objective value from among all the initial particle positions.

Moreover, the computational complexity of PSO is based on the number of particles, R_p, and the total number of iterations, I_{PSO}^{total}[30]. Thus, the total complexity of the proposed PSO scheme is $\mathcal{O}\left(R_p \cdot I_{PSO}^{total}\right)$.

3) CS-BASED FRAMEWORK WITH LÉVY FLIGHTS FOR TRANSMISSION POWER MINIMIZATION

The CS algorithm was inspired by the brood parasitism of the cuckoo species, laying their eggs in the nests of other birds. However, when a host bird realizes the eggs are not its own, it will either leave its nest and build a new one or push the intruding cuckoo's eggs out of the nest. This action can be represented by probability $p_a \in [0, 1]$.

Some cuckoo species are able to mimic the pattern and color of the eggs of a few select host species. This is a key feature that increases cuckoo chick reproduction and prevents them from being abandoned. Overall, the advantage is that the cuckoo eggs hatch slightly earlier than the host eggs, and once the first cuckoo chick emerges, its first act is to dislodge the host species' eggs. This increases its access to feeding opportunities [31].

The main idea is that each egg in a nest represents a solution, and the nests with high-quality eggs, i.e., those with potentially the best solutions, will replace a not-so-good solution in the nest and will be carried over to the next generation. In this paper, we assume each nest has one egg.

Then, each egg is a vector of four elements, p_1, p_2, α, and τ, that are the variables to be optimized, $\mathbf{q}_n = \{p_{1,n}, p_{2,n}, \alpha_n, \tau_n\}$, where $n = 1, 2, 3, \ldots, N$, in which N denotes the number of nests. Similar to equation (17), indicated in the PSO-based algorithm, we use a penalty function to deal with constraints, as follows:

$$f(\mathbf{q}_n) = p_1 + p_2 + \varsigma \sum_{i=1}^{4} \xi(g_i). \tag{20}$$

Algorithm 1 The Proposed PSO-Based Algorithm to Solve Problem (14)

1: Establish the input parameters of PSO.
2: Set iteration counter $t = 1$.
3: Initialize particle positions that are randomly selected according to the feasible search region $[0, P^{\max}]$, and $(0, 1)$. $\mathbf{q}^t = \left\{\left(q_{p_1,1}^t, q_{p_2,1}^t, q_{\alpha,1}^t, q_{\tau,1}^t\right), \ldots, \left(q_{p_1,R_p}^t, q_{p_2,R_p}^t, q_{\alpha,R_p}^t, q_{\tau,R_p}^t\right)\right\}$
4: Initialize the particles' velocities: $\mathbf{v}^t = \left(\mathbf{v}_1^t, \mathbf{v}_2^t, \ldots, v_r^t\right)$
5: Calculate minimum transmission power $f\left(\mathbf{q}_r^t\right)$ by evaluating (17) for each r-th particle.
6: Set the initial best particles' positions, $\forall r$. $\mathbf{lb}_r^t = \mathbf{q}_r^t$.
7: Set the initial global best position, $\mathbf{gb}^t = \arg\min_{1 \le r \le R_p} f\left(\mathbf{lb}_r^t\right)$.
8: **For** each particle r **do**
9: From (18), update the particles' velocities.
10: From (19), update the particles' positions.
11: Update the best particles' positions,
if $f\left(\mathbf{q}_r^{t+1}\right) < f\left(\mathbf{lb}_r^t\right)$ **then**
$\mathbf{lb}_r^{t+1} = \mathbf{q}_r^{t+1}$
else
$\mathbf{lb}_r^{t+1} = \mathbf{lb}_r^t$
end if
12: **end for**
13: Update the global best particles' positions, $\mathbf{gb}^{t+1} = \arg\min_{1 \le r \le R_p} f\left(\mathbf{lb}_r^{t+1}\right)$.
14: **if** $t < I_{PSO}^{total}$, **then**
$t = t + 1$ and go to Step 8
else
go to Step 15
end if
15: **Return:** the best values of resource allocation variables, $\left\{p_1^*, p_2^*, \alpha^*, \tau^*\right\} = \mathbf{gb}$, to obtain the minimum value of total transmission power indicated in problem (14).

Then, each solution, $f(\mathbf{q}_n)$, is based on the objective function of problem (14), which aims to minimize total transmission power. After that, the generation of new solutions is carried out by Lévy flights [19-21]. For instance, the procedure in Lévy flights to generate a new solution for power allocation variable p_1 can be expressed as follows:

$$p_1^{t,new} = p_1^t + R \cdot \beta \cdot L(s,\lambda)\left(p_1^t - p_{1,g}^t\right), \tag{21}$$

where R is random number $\mathcal{N}(0,1)$, $p_{1,g}^t$ is the nest with the best fitness function, $L(s,\lambda) = \frac{\lambda\Gamma(\lambda)\sin(\pi\lambda/2)}{\pi}\frac{1}{s^{1+\lambda}}$, $\beta > 0$ is the step size, and factor $1 < \lambda \leq 3$ we consider to have a value of $\lambda = 3/2$. Parameter s denotes the step length based on Mantegna's algorithm [32], and it can be calculated by

$$s = \frac{u}{|\upsilon|^{1/\beta}}, \tag{22}$$

where $u \sim \mathcal{N}\left(0,\sigma_u^2\right)$, $\upsilon \sim \mathcal{N}\left(0,\sigma_\upsilon^2\right)$, $\sigma_u^2 = \left\{\frac{\Gamma(1+\lambda)\sin(\pi\lambda/2)}{\Gamma[(1+\lambda)/2]\lambda 2^{(\lambda-1)/2}}\right\}$, $\sigma_\upsilon^2 = 1$.

Similarly, the process to compute the new solution for power allocation variables p_2, α, and τ can be written as

$$p_2^{t,new} = p_2^t + R \cdot \beta \cdot L(s,\lambda)\left(p_2^t - p_{2,g}^t\right), \tag{23}$$

$$\alpha^{t,new} = \alpha^t + R \cdot \beta \cdot L(s,\lambda)\left(\alpha^t - \alpha_g^t\right), \tag{24}$$

and

$$\tau^{t,new} = \tau^t + R \cdot \beta \cdot L(s,\lambda)\left(\tau^t - \tau_g^t\right). \tag{25}$$

For simplicity, we denote that $\mathbf{q}_g^t = \left\{p_{1,g}^t, p_{2,g}^t, \alpha_g^t, \tau_g^t\right\}$. It is worth mentioning that in this paper, we implement an improved CS version described in [26]. In the conventional CS algorithm, the probability, p_a, and the step size, β, are fixed parameters. However, fine-tuning these parameters can be essential to enhancing the convergence rate and the performance of the algorithm. Therefore, we implemented the improved CS version, which dynamically changed the parameters, p_a and β, based on the number of generations. Accordingly, probability p_a was modified as follows:

$$p_a = p_a^{\max} - \frac{t}{I_{CS}^{total}}\left(p_a^{\max} - p_a^{\min}\right), \tag{26}$$

where t denotes the current iteration, and I_{CS}^{total} denotes the total number of iterations. According to the experiment results, we consider $p_a^{\max} = 0.5$, and $p_a^{\min} = 0.25$.

Moreover, step size parameter β is modified as follows:

$$\beta = \beta_{\max}\exp(q \cdot t), \tag{27}$$

where $q = \frac{1}{I_{CS}^{total}}\ln\left(\frac{\beta_{\min}}{\beta_{\max}}\right)$. A fraction of the worst nests, p_a, are abandoned and their positions are updated as follows [28]:

$$p_1^{t,new} = p_1^t + R \cdot \left(p_{1,g}^t - p_{1,u}^t\right), \tag{28}$$

$$p_2^{t,new} = p_2^t + R \cdot \left(p_{2,g}^t - p_{2,u}^t\right), \tag{29}$$

$$\alpha^{t,new} = \alpha^t + R \cdot \left(\alpha_g^t - \alpha_u^t\right), \tag{30}$$

$$\tau^{t,new} = \tau^t + R \cdot \left(\tau_g^t - \tau_u^t\right), \tag{31}$$

where $\mathbf{q}_u^t = \left\{p_{1,u}^t, p_{2,u}^t, \alpha_u^t, \tau_u^t\right\}$ is a randomly selected nest.

The procedure of the CS-based algorithm in solving power minimization problem (14) is described in Algorithm 2. The input parameters are the maximum transmission power at the transmitter, $P^{\max}$; the target rate value of user 1, γ_1; the target rate value of user 2, γ_2; the minimum energy harvesting at user 3, ϕ; the maximum iteration number, I_{CS}^{total}; the number of nests, denoted by N; the probability that a host bird discovers the intruder cuckoo's egg, p_a; step size β, factor λ, and step length s. In addition, as input parameters, the lower and upper boundaries of the variables to be optimized are considered. Then, power allocation variables p_1 and p_2 are within the range $[0, P^{\max}]$, while variables for fraction transmission time τ and power splitting ratio β fall within $(0,1)$. Moreover, the computational complexity of the CS depends on the number of nests, N, and the total number of iterations, I_{CS}^{total} [33]. Thus, the total complexity of the CS scheme is $\mathcal{O}\left(N \cdot I_{CS}^{total}\right)$.

B. ENERGY EFFICIENCY OPTIMIZATION PROBLEM

In this problem, we aim to maximize the total energy efficiency of the proposed cooperative non-linear SWIPT-enabled NOMA system that also considers an additional non-linear EH user. Here, we jointly optimized the transmission time fraction, τ, the power-splitting ratio, α, and the power allocation variables, p_1 and p_2, while satisfying the QoS constraints of all users. The energy efficiency is defined as the ratio of total rate to power consumption, as shown in the objective function of the problem, and it can be formulated as follows:

$$\max_{p_1,p_2,\tau,\alpha} \frac{R_{u_1} + R_{u_2}}{\tau(p_1 + p_2 + p_{c1}) + (1-\tau)(P_{sw} + p_{c2})}$$
$$\text{s.t. } (14b), (14c), (14d), (14e), (14f), (14g), (14h), \tag{32a}$$

where $R_{u1} = \min\left(R_{x_1,u_2}^{(1)}, R_{x_1,u_1}^{(2)}\right)$, p_{c1} and p_{c2} are the circuit power variables at user 1 and user 2, respectively.

It is worth highlighting that the energy efficiency maximization problem is more challenging to solve since the cost function is in fractional form and constraints are non-convex. Therefore, in Subsection III.B.1, we propose a swarm-intelligence-based scheme called PSO to reduce the computational complexity, and in Subsection III.B.2, we develop a CS-based benchmark scheme for comparison purposes.

1) PROPOSED PSO-BASED FRAMEWORK FOR ENERGY EFFICIENCY MAXIMIZATION

Similar to (16), we define the objective function as follows:

$$f(\mathbf{q}_n) = \frac{R_{u_1} + R_{u_2}}{\tau(p_1 + p_2 + p_{c1}) + (1-\tau)(P_{sw} + p_{c2})} - \varsigma\sum_{i=1}^{4}\xi(g_i). \tag{33}$$

Algorithm 2 CS-Based Framework to Solve Power Minimization Problem (14)

1: Input parameters of CS scheme.
2: Objective function $f(\mathbf{q}_n)$ in (20).
3: Initialize a population of N host nests for each variable to be optimized, $\mathbf{q}_n = \{p_{1,n}, p_{2,n}, \alpha_n, \tau_n\}$, $n \in \{1, .2, \ldots, N\}$.
4: Initialize $t = 0$.
5: Evaluate fitness function for each nest, $F_n^t = f\left(\mathbf{q}_n^t\right), \forall n$, and find $\mathbf{q}_g^t$.
6: **For** $t < I_{CS}^{total}$ **do**
7: Calculate β with (27) and obtain new position $\mathbf{q}_n^{t,new} = \left\{p_{1,n}^{t,new}, p_{1,n}^{t,new}, \alpha_{1,n}^{t,new}, \tau_n^{t,new}\right\}$ for each nest via Lévy flights with (21), (23), (24), and (25).
8: Evaluate the fitness function for each nest, $F_n^{t,new}, \forall n$.
9: For all nests do:
if $F_n^{t,new} < F_n^t$
$F_n^{t+1} = F_n^{t,new}$, $\mathbf{q}_n^{t+1} = \mathbf{q}_n^{t,new}$
else
$F_n^{t+1} = F_n^t$, $\mathbf{q}_n^{t+1} = \mathbf{q}_n^t$
end if
10: Calculate the value of p_a with (26).
11: A fraction, p_a, of the worst nests are abandoned, and the corresponding positions of the nests are updated based on (28)-(31).
12: Evaluate fitness of new nests and execute Step 9; rank all solutions and find the current best nest.
13: $t = t + 1$
14: **end for**
15: **Return:** the best values, $\left\{p_1^*, p_2^*, \alpha^*, \tau^*\right\}$ = **best_nest**, to obtain the minimum transmission power indicated in problem (14).

Then, the PSO algorithm to solve problem (32) is based on Algorithm 1 with the following modifications: (a) the objective function is evaluated with (33); (b) the global best position is obtained with $\mathbf{gb}^t = \arg\max_{1 \le r \le R_p} f\left(\mathbf{lb}_r^t\right)$; (c) in Step 11, the condition to update the local best position is $f\left(\mathbf{q}_r^{t+1}\right) > f\left(\mathbf{lb}_r^t\right)$.

2) CUCKOO-SEARCH-BASED FRAMEWORK WITH LÉVY FLIGHTS FOR ENERGY EFFICIENCY MAXIMIZATION

To maximize the energy efficiency of the proposed NOMA SWIPT network based on CS with Lévy flights, we follow Algorithm 2 with minor modifications. Since the current optimization problem is one of maximization, in Step 9 of Algorithm 2, we replace inequality $F_n^{t,new} < F_n^t$ with $F_n^{t,new} > F_n^t$. In addition, the objective function is given in (33). Then, we obtain the best values, $\left\{p_1^*, p_2^*, \alpha^*, \tau^*\right\}$ = **best_nest**, to achieve the maximum energy efficiency indicated in (32a).

IV. NUMERICAL RESULTS

In this section, we present the simulation results programmed into MATLAB software, of the proposed cooperative nonlinear SWIPT-enabled NOMA system. The results are averaged over several channel realizations. More specifically, we present a performance comparison between the optimal scheme provided by the convex optimization with the ES method, denoted as CVX+ES, and the proposed PSO-based scheme. Moreover, we assess the performance of the following swarm intelligence-based baseline algorithms: CS, the ant lion optimization (ALO) method, the butterfly optimization algorithm (BOA), the firefly algorithm (FA), and the bat algorithm (BA). In addition, we compare the performances between NOMA and OMA transmission cooperative communication with a TF scheme ($\tau = 0.5$) [35]–[39], and SWIPT NOMA cooperative communication with the EPS scheme ($\alpha = 0.5$) [15].

Rayleigh fading channels $\widetilde{k_2}, \widetilde{f}, \widetilde{e}$ have i.i.d. complex Gaussian entries with zero mean and a certain variance, i.e, $\widetilde{k_2} \sim \mathcal{CN}\left(0, d_{t_r u_2}^{-pl}\right), \widetilde{f} \sim \mathcal{CN}\left(0, d_{u_1 u_2}^{-pl}\right)$, and $\widetilde{e} \sim \mathcal{CN}\left(0, d_{t_r u_3}^{-pl}\right)$, respectively, where d_{ij} denotes the distance between nodes i and j, and pl is the path-loss exponent; index t_r indicates the transmitter. In the simulations, we assume the path-loss exponent is $pl = 2$ for channels $\widetilde{k_2}, \widetilde{f}, \widetilde{e}$, and noise power is $\sigma_1^2 = \sigma_2^2 = -60$ dBm. The distances in meters between the nodes are $d_{t_r u_2} = 15$, $d_{u_1 u_2} = 18$, and $d_{t_r u_3} = 6$. Moreover, the maximum transmission power at the transmitter is $P^{\max} = 30$ dBm.

A. TRANSMISSION POWER MINIMIZATION

In this subsection, we analyze the numerical results obtained for transmission power minimization. Figure 3 shows the total transmit power of the proposed PSO-based scheme compared with those of the following swarm intelligence algorithms: CS, ALO, BAO, FA, and BA. The parameters of each algorithm in Table 1 are set based on the best results achieved through several experiments. The description of these baseline swarm algorithms and their parameters are explained in [40]. From Figure 3, it is observed that the trend of all schemes rises as the minimum rate at user 1 increases. However, the proposed PSO scheme outperforms the comparison swarm intelligent algorithms in terms of total transmit power. It is noteworthy that the performance of CS is very close to that obtained by PSO. Thus, to validate the superiority of PSO, we evaluate the convergence behavior between PSO and CS. In addition, we compare the average (central processing unit) CPU running time of the proposed PSO-based framework, the optimal CVX+ES method, and the performance of five benchmark swarm intelligence algorithms.

Figure 4 illustrates the convergence behavior of the proposed low-complexity PSO algorithm and the CS baseline algorithm according to the number of iterations. We can see that as the number of iterations increases, the total transmission power is minimized. Moreover, Figure 4 shows

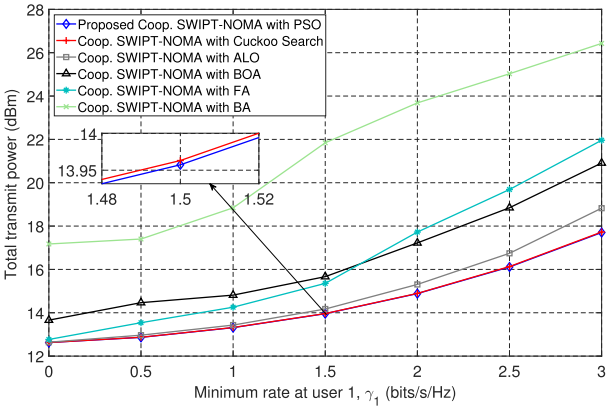

FIGURE 3. Total transmit power of the proposed PSO-based scheme, CS, ALO, BOA, FA, and BA according to the minimum rate at user 1, γ_1.

TABLE 1. Simulation parameters for transmission power minimization.

Algorithm	Simulation parameters
PSO	$I_{PSO}^{total} = 60$ $R_p = 30$ $Ine = 0.7$ $c_1 = 1.494$ $c_2 = 1.494$
CS	$I_{CS}^{total} = 250$ $N = 35$ $\beta_{\min} = 0.01$ $\beta_{\max} = 0.5$
ALO	Number of iterations, $I_{ALO}^{total} = 120$ Number of ants, $N_{ALO} = 30$
BOA	Number of generations, $G_{BOA} = 250$ Number of agents, $S_{BOA} = 35$ Sensory modality, $sm = 0.01$ Power exponent, $pe = 0.01$ Switch probability, $sp = 0.5$
FA	Number of iterations, $I_{FA}^{total} = 500$ Number of fireflies, $N_{FA} = 40$ Randomness strength, $R_{str} = 1$ Attractiveness constant, $Atc = 1$ Absorption coefficient, $ac = 0.01$ Randomness reduction factor, $R_{rf} = 0.97$
BA	Number of iterations, $I_{BA}^{total} = 200$ Number of bats, $N_{BA} = 40$ Pulse emission rate, $p_{BA} = 0.001$ Maximum frequency, $f_{BA}^{\max} = 2$ Minimum frequency, $f_{BA}^{\min} = 0$ Constant for loudness, $l_{BA} = 0.5$ Constant for emission rate, $l_{er} = 0.5$

that for the PSO-based scheme, the transmit power converges within about 60 iterations. Therefore, we fix the number of iterations, I_{PSO}^{total}, equal to 60 at other simulations. Moreover, we also set the number of particles at $R_p = 30$, the inertia weight to $Ine = 0.7$, along with the scaling factors, $c_1 = 1.494$, and $c_2 = 1.494$. Meanwhile, for the CS-based scheme, Figure 4 shows that the transmit power converges within about 250 iterations, which is a bit more than double that of PSO and entails higher complexity. After the fine-tuning process for CS, we set its parameters: number of nests, $N = 35$, and total iterations, $I_{CS}^{total} = 250$. Furthermore, we can see that total transmission power increases as the minimum requirement for EH at u_3, and the minimum target rates, γ_1 and γ_2, respectively, increases. This is because more

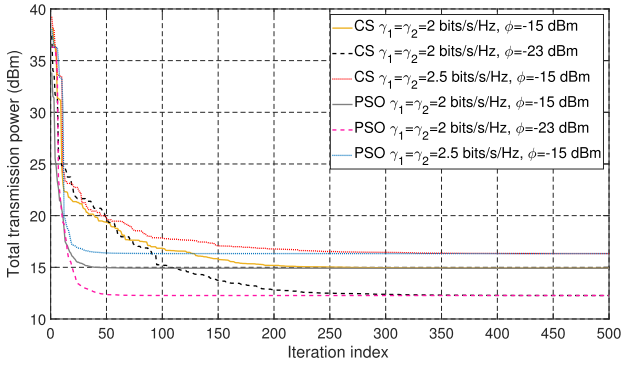

FIGURE 4. Convergence of the proposed PSO-based algorithm and CS with different required rates γ_1, γ_2, and minimum harvested energy, ϕ, for transmission power minimization.

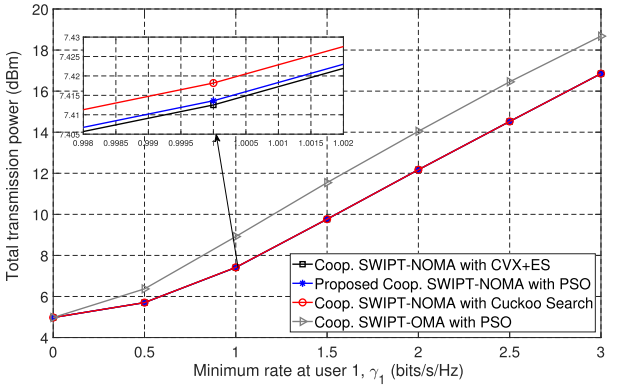

FIGURE 5. Performance comparison among the optimal scheme (CVX+ES), the PSO-based scheme, the CS-based scheme, and cooperative SWIPT-OMA for transmission power minimization.

power must be allocated to users as the QoS requirements increase.

To validate the optimality of the proposed low-complexity PSO-based framework, Figure 5 shows the performance comparison between the optimal scheme, CVX+ES, the PSO-based scheme, the CS-based scheme, and cooperative SWIPT-OMA for transmission power minimization. Note that CVX with the ES method corresponds to the analytical solution indicated in subsection III.A. Figure 5 shows the transmission power when the minimum EH requirement is $\phi = -23$dBm, and target rate at u_2 is $\gamma_2 = 1$ bit/s/Hz. From Figure 5, we verify that the proposed PSO and CS-based frameworks provide near-optimal performance, compared with the CVX+ES method. In addition, it is worth highlighting that the PSO-based scheme can reach a result closer to the optimal solution provided by CVX+ES in fewer iterations than under the CS, which means that less time is needed to compute a solution with higher performance. Therefore, in this paper, we propose the PSO-based framework as the most suitable low-complexity solution in the cooperative non-linear SWIPT-NOMA network.

TABLE 2. CPU running time.

Scheme	CPU time (sec)
PSO	0.671
CVX+ES	3584
CS	6.017
ALO	3.495
BOA	25.106
FA	119.641
BA	2.784

Furthermore, the average CPU running times are compared in Table 2 among the proposed PSO-based framework, the optimal CVX+ES method, and five benchmark swarm intelligence algorithms. The results are obtained by using a computer with a 4 GHz i7-6700K CPU and 16 GB RAM. Firstly, we can observe that CVX+ES requires the most computation time. By contrast, the low-complexity solutions provided by the proposed PSO-based scheme and the swarm intelligence-based baseline algorithms can reduce the CPU running time to obtain a sub-optimal solution. However, it is remarkable that the PSO scheme requires the least CPU running time to reach a solution than their counterparts to reach a solution. This is because PSO requires fewer iterations compared to the benchmark swarm intelligence schemes, as shown in Table 1. Particularly, from Figure 5, we can observe that CS and PS achieve a very close performance to the optimal CVX+ES method. However, we can also see that CS needs more time than PSO to reach a solution. This is because PSO requires fewer iterations to achieve convergence compared to the CS method. Moreover, the number of particles, R_p, utilized in PSO is lower than the number of nests, N, required under CS. Recall that the computation complexity depends on the number of iterations and the number of particles used by each algorithm. Specifically, the computational complexity of PSO is computed by $\mathcal{O}\left(R_p \cdot I_{PSO}^{total}\right)$ while the computation complexity of CS is computed by $\mathcal{O}\left(N \cdot I_{CS}^{total}\right)$. In this sense, since the PSO-based scheme requires fewer iterations and a lower number of particles than that required by CS, the least computational complexity with the highest accuracy is achieved by the proposed PSO-based solution. Regarding CVX+ES, the problem (15) should be solved for each possible time value for τ and it is needed to check if the candidate solution satisfies all the constraints. Next, the candidate solution with the lowest objective function is defined as the best solution. Then, the CVX+ES method cannot have a convergence behavior like the presented in Figure 4 for PSO and CS because the possible values of τ are tested in order from 0 to 1 with a predefined step. For instance, we considered increments of 0.0001 for τ, and thus, solved the problem (15) a total of 10,000 times, whereas the average time to solve the problem (15) is 0.358 sec.

Moreover, we considered the total power minimization problem for the cooperative non-linear SWIPT-enabled OMA benchmark. We used the time-division multiplexing (TDMA) technique in which three phases are required to complete transmission in the comparison SWIPT-OMA scheme. Specifically, TDMA allocates a fraction of time τ_1 and τ_2 to u_1 and u_2, respectively. Moreover, a fraction of time τ_3 is assigned to the cooperative transmission from u_2 to u_1. From Figure 5, we observed that the proposed cooperative SWIPT-NOMA scheme outperforms the conventional OMA strategy in the cooperative network since OMA increases the total transmission power compared with the proposed cooperative NOMA scheme. This is because, in NOMA, the users share the same frequency at the same time, which improves the spectral efficiency of the system. By contrast, OMA requires more resources to complete a transmission because users share the same frequency channel at different times.

Figure 6 and Figure 7 illustrate the effect from linearity of EH on the transmit power of the proposed scheme (cooperative SWIPT NOMA communication optimizing resource allocation variables p_1, p_2, τ, and α) and the following baseline schemes: SWIPT NOMA cooperative communication with TF, and SWIPT NOMA cooperative communication with EPS. In cooperative non-linear SWIP-NOMA, we used the non-linear EH model at u_2 specified in (7) and the non-linear EH model at u_3 specified in (9). On the other hand, for application of the ideal linear EH model in the cooperative SWIPT-enabled NOMA system, we used the linear EH model at u_2 specified in (6) and the linear EH model at u_3 specified in (10). Moreover, we considered $\eta = 1$ for the linear EH models. Overall, we verified that the cooperative SWIPT-NOMA scheme with a linear EH model achieved lower transmission power since it considers the users to be storing all the power of the incoming signal. By contrast, the non-linear EH model considers a more realistic environment where the relationship between stored energy and received RF power is non-linear because of physical impairments, saturated harvested power, and circuit specifications. Moreover, from Figure 6 and Figure 7, we can see that the proposed cooperative non-linear SWIPT-NOMA scheme outperforms the EPS and TF baseline schemes. This verifies that including the power splitting ratio and time fraction variables in the optimization problem improves the performance of the network. Recall that the EPS and TF schemes considered the power splitting ratio to be $\alpha = 0.5$, and the time transmission fraction to be set at $\tau = 0.5$, respectively.

B. ENERGY EFFICIENCY MAXIMIZATION

In this subsection, we assess the results for energy efficiency maximization in the proposed nonlinear SWIPT NOMA system.

Figure 8 shows energy efficiency among the proposed PSO-based scheme and the following swarm intelligence algorithms: CS, ALO, the BAO, FA, and BA. The parameters of each algorithm in Table 3 are set based on the best results achieved through several experiments. From Figure 8, it is observed that the energy efficiency of all schemes diminishes as the minimum rate at user 1 increases. However, the proposed PSO scheme outperforms the other

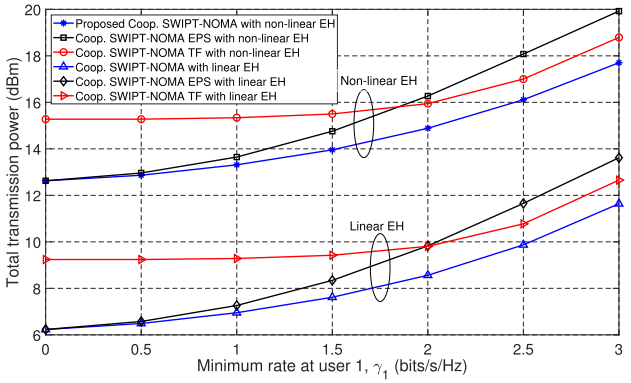

FIGURE 6. Transmit power comparison between the proposed cooperative non-linear SWIPT-NOMA and cooperative linear SWIPT-NOMA according to different required rate, γ_1, $\gamma_2 = 1$ bit/s/Hz, $\phi = -15$ dBm.

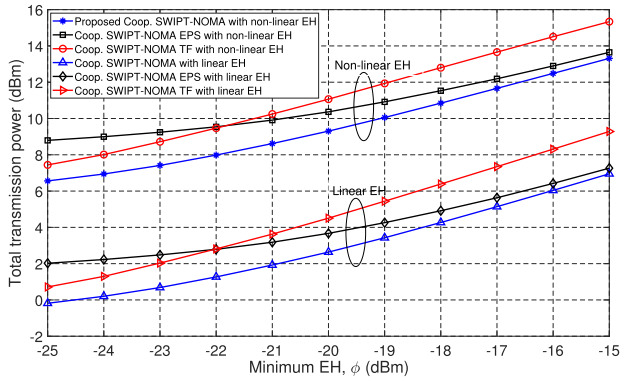

FIGURE 7. Transmit power comparison between the proposed cooperative non-linear SWIPT-NOMA and cooperative linear SWIPT-NOMA according to different required EH, ϕ, $\gamma_1 = 1$ bit/s/Hz, $\gamma_2 = 1$ bit/s/Hz.

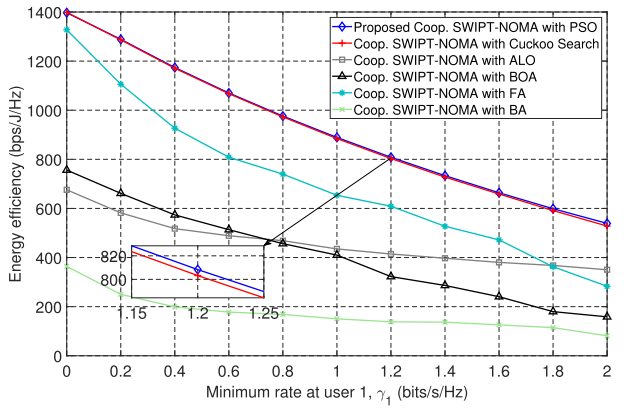

FIGURE 8. Energy efficiency comparison among the proposed PSO-based scheme, CS, ALO, BOA, FA, and BA according to the minimum rate at user 1, γ_1.

swarm intelligent algorithms by utilizing fewer iterations to obtain the maximum energy efficiency which entails less computational time. Similar to the transmit power problem, the performance of CS is very close to that obtained by PSO. Thus, to validate the superiority of PSO, we evaluate

TABLE 3. Simulation parameters for energy efficiency.

Algorithm	Simulation parameters
PSO	$I_{PSO}^{total} = 125$ $R_p = 35$ $Ine = 0.7$ $c_1 = 1.494$ $c_2 = 1.494$
CS	$I_{CS}^{total} = 400$ $N = 35$ $\beta_{\min} = 0.01$ $\beta_{\max} = 0.5$
ALO	$I_{ALO}^{total} = 250$ $N_{ALO} = 35$
BOA	$G_{BOA} = 250$ $S_{BOA} = 60$ $sm = 0.01$ $pe = 0.01$ $sp = 0.5$
FA	$I_{FA}^{total} = 500$ $N_{FA} = 60$ $R_{str} = 1$ $Atc = 1$ $ac = 0.01$ $R_{rf} = 0.97$
BA	$I_{BA}^{total} = 250$ $N_{BA} = 50$ $p_{BA} = 0.001$ $f_{BA}^{\max} = 2$ $f_{BA}^{\min} = 0$ $l_{BA} = 0.5$ $l_{er} = 0.5$

the convergence behavior and the CPU time between PSO and CS.

Figure 9 illustrates the convergence behavior of energy efficiency of the proposed low-complexity PSO-based algorithm and the CS baseline scheme. As the number of iterations increases, energy efficiency is maximized. Moreover, Figure 9 shows that in the case of PSO, the energy efficiency is converged within about 125 iterations. Therefore, we set the number of iterations, I_{PSO}^{total}, at 125. Moreover, we set the number of particles to $R_p = 35$, the inertia weight to $Ine = 0.7$, and for the scaling factors, $c_1 = 1.494$, and $c_2 = 1.494$. Regarding CS, from Figure 9, we can see that the energy efficiency is converged within about 400 iterations. Similar to the convergence behavior for the power minimization problem, the number of iterations for energy efficiency is also more than double that of PSO, which entails higher complexity. After performing various experiments with CS, we selected the parameters for the number of nests, $N = 35$, and the total iterations, $I_{CS}^{total} = 400$. Moreover, from Figure 11, we can see that the energy efficiency decreases as the minimum requirements for EH at u_3, and for the minimum target rates, γ_1 and γ_2, increase. This is because when QoS requirements increase, more power needs to be allocated to users. Accordingly, energy efficiency is reduced, since its relationship to power consumption is inversely proportional.

From Figure 10, we verified that the energy efficiency performances obtained by the proposed PSO- and CS-based frameworks are close to that by the ES method with the minimum EH requirement, $\phi = -23$ dBm, and for the

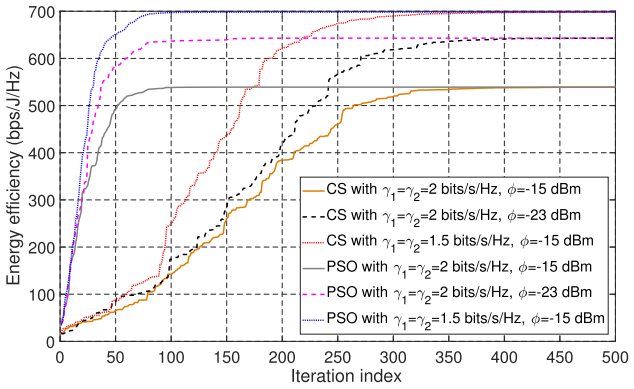

FIGURE 9. Convergence of the proposed PSO-based algorithm and CS with different required rates, γ_1, γ_2, and minimum harvesting energy, ϕ, for energy efficiency maximization.

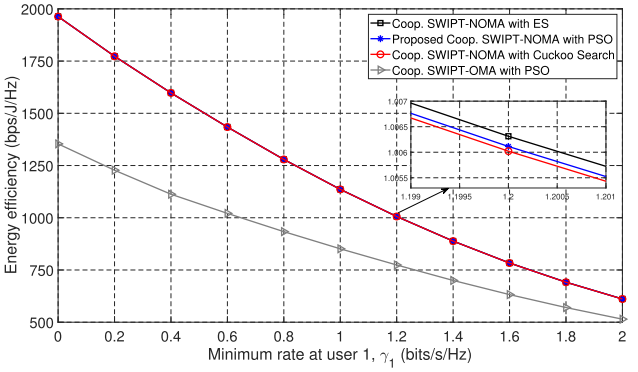

FIGURE 10. Energy efficiency performance of ES, cooperative non-linear SWIPT-NOMA with PSO, cooperative non-linear SWIPT-NOMA with CS, and cooperative non-linear SWIPT-OMA with PSO.

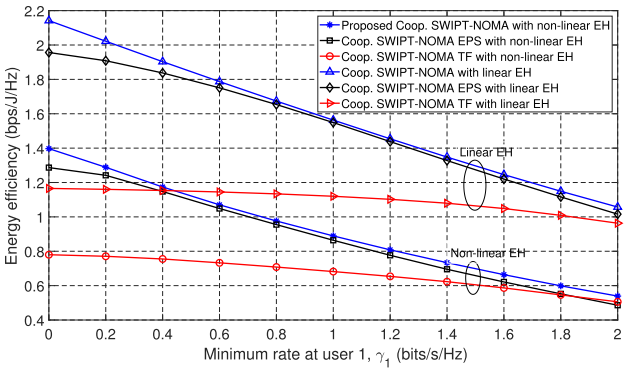

FIGURE 11. Energy efficiency comparison between the proposed cooperative non-linear SWIPT-NOMA, and cooperative linear SWIPT-NOMA according to different required rates, γ_1, $\gamma_2 = 1$ bit/s/Hz, $\phi = -15$ dBm.

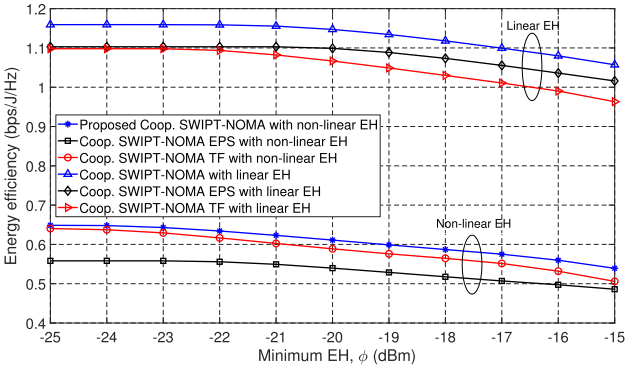

FIGURE 12. Energy efficiency comparison between the proposed cooperative non-linear SWIPT-NOMA, and cooperative linear SWIPT-NOMA according to different required EH, ϕ, $\gamma_1 = 1$ bit/s/Hz, $\gamma_2 = 1$ bit/s/Hz.

target rate at u_2, $\gamma_2 = 1$ bit/s/Hz. In contrast to the ES method, the low-complexity solutions provided by PSO and CS can lessen the time needed to achieve an approximately optimal solution with low computational complexity. It is worth noting that the proposed PSO-based scheme can reach a result closer to the optimal solution provided by ES in fewer iterations than the CS-based scheme. This means less time is needed to compute a solution with higher performance. Therefore, we propose the PSO-based scheme as a powerful low-complexity solution in cooperative non-linear SWIPT-NOMA networks. Moreover, from Figure 10, we verify that the proposed cooperative SWIPT-NOMA network outperforms the OMA scheme in terms of energy efficiency.

Figure 11 and Figure 12 illustrate the effect from linearity of EH on energy efficiency in the proposed cooperative SWIPT NOMA communication that optimizes the variables p_1, p_2, τ, and α, and on the following baseline schemes: SWIPT NOMA cooperative communications with a TF scheme, and SWIPT NOMA cooperative communications with EPS. Besides, we consider $\eta = 1$. From Figure 11 and Figure 12, we verify that the cooperative SWIPT-NOMA scheme with the ideal linear EH model achieves higher energy efficiency. This is due to a linear relationship between the stored energy and the received RF power. Thus, users can store all the power of the incoming signal. This differs from the proposed non-linear EH model, which considers a more realistic environment that involves saturated harvested power and circuit specifications. Furthermore, from Figure 11 and Figure 10, we can see that the proposed cooperative non-linear SWIPT-NOMA scheme outperforms the EPS and TF baseline schemes in terms of energy efficiency.

V. CONCLUSION

In this paper, we propose to optimize transmission power and energy efficiency in a collaborative non-linear SWIPT-NOMA system with a non-linear EH user while satisfying constraints on minimum target rate at the users and minimum harvested energy at the terminal. The considered optimization problems are non-convex, involving joint optimization of the transmission time fraction, the power splitting ratio, and power allocation, and are thus difficult to solve directly. To tackle this issue, we propose a PSO–based solution with low computational complexity where results reach performance near-optimal to those obtained by the optimal

but time- and energy-consuming convex optimization and ES methods. In addition, we also study and develop a CS-based benchmark as an alternative low-complexity solution and evaluate the performance of five swarm intelligence benchmark schemes. Simulation results showed that PSO requires fewer iterations than the swarm intelligence baseline schemes to achieve convergence, which leads to the least CPU time for PSO. Furthermore, we investigate cooperative non-linear SWIPT-OMA, EPS, and TF benchmark schemes for performance comparison with the proposed cooperative non-linear SWIPT-NOMA system. Results showed that the proposed cooperative non-linear NOMA with SWIPT can reduce transmit power and achieved higher spectral efficiency compared to the OMA, EPS, and TF baseline schemes. It is worth highlighting that the optimization of the time variable provided a significant performance improvement, but it is conventionally kept as a constant in the literature. Furthermore, we analyzed the application of a non-linear EH model with the ideal linear EH. The developed schemes with linear EH achieved lower transmission power and high energy efficiency because they consider an ideal case where the receiver harvests all the power of the incoming signal.

REFERENCES

[1] G. Chen, J. Tang, and J. P. Coon, "Optimal routing for multihop social-based D2D communications in the Internet of Things," *IEEE Internet Things J.*, vol. 5, no. 3, pp. 1880–1889, Jun. 2018.

[2] C. E. Garcia, M. R. Camana, and I. Koo, "Particle swarm optimization-based secure computation efficiency maximization in a power beacon-assisted wireless-powered mobile edge computing NOMA system," *Energies*, vol. 13, no. 21, p. 5540, Oct. 2020.

[3] H. J. Visser and R. J. M. Vullers, "RF energy harvesting and transport for wireless sensor network applications: Principles and requirements," *Proc. IEEE*, vol. 101, no. 6, pp. 1410–1423, Jun. 2013.

[4] M.-L. Ku, W. Li, Y. Chen, and K. J. R. Liu, "Advances in energy harvesting communications: Past, present, and future challenges," *IEEE Commun. Surveys Tuts.*, vol. 18, no. 2, pp. 1384–1412, 2nd Quart. 2016.

[5] S. Ulukus, "Energy harvesting wireless communications: A review of recent advances," *IEEE J. Sel. Areas Commun.*, vol. 33, no. 3, pp. 360–381, Apr. 2015.

[6] X. Lu, P. Wang, D. Niyato, D. I. Kim, and Z. Han, "Wireless networks with RF energy harvesting: A contemporary survey," *IEEE Commun. Surveys Tuts.*, vol. 17, no. 2, pp. 757–789, 2nd Quart., 2015.

[7] J. Luo, J. Tang, D. K. C. So, G. Chen, K. Cumanan, and J. A. Chambers, "A deep learning-based approach to power minimization in multi-carrier NOMA with SWIPT," *IEEE Trans. Signal Process.*, vol. 7, pp. 17450–17460, 2019.

[8] A. Pop-Vadean, P. P. Pop, T. Latinovic, C. Barz, and C. Lung, "Harvesting energy an sustainable power source, replace batteries for powering WSN and devices on the IoT," *IOP Conf. Ser., Mater. Sci. Eng.*, vol. 200, Sep. 2017, Art. no. 012043.

[9] K. Xiong, B. Wang, and K. J. R. Liu, "Rate-energy region of SWIPT for MIMO broadcasting under nonlinear energy harvesting model," *IEEE Trans. Wireless Commun.*, vol. 16, no. 8, pp. 5147–5161, Aug. 2017.

[10] K. Ali, H. X. Nguyen, Q. Vien, P. Shah, and Z. Chu, "Disaster management using D2D communication with power transfer and clustering techniques," *IEEE Access*, vol. 6, pp. 14643–14654, 2018.

[11] J. Tang, J. Luo, M. Liu, D. K. C. So, E. Alsusa, G. Chen, K.-K. Wong, and J. A. Chambers, "Energy efficiency optimization for NOMA with SWIPT," *IEEE J. Sel. Topics Signal Process.*, vol. 13, no. 3, pp. 452–466, Jun. 2019.

[12] Z. Wang and Q. Zhu, "Energy efficiency optimization algorithm of CR-NOMA system based on SWIPT," *Math. Problems Eng.*, vol. 2020, pp. 1–13, Jun. 2020.

[13] Y. Yuan, Y. Xu, Z. Yang, P. Xu, and Z. Ding, "Energy efficiency optimization in full-duplex user-aided cooperative SWIPT NOMA systems," *IEEE Trans. Commun.*, vol. 67, no. 8, pp. 5753–5767, Aug. 2019.

[14] S. Mao, S. Leng, J. Hu, and K. Yang, "Power minimization resource allocation for underlay MISO-NOMA SWIPT systems," *IEEE Access*, vol. 7, pp. 17247–17255, 2019.

[15] C. E. Garcia, P. V. Tuan, M. R. Camana, and I. Koo, "Optimized power allocation for a cooperative NOMA system with SWIPT and an energy-harvesting user," *Int. J. Electron.*, vol. 107, no. 10, pp. 1704–1733, May 2020.

[16] J. Tang, T. Dai, M. Cui, X. Y. Zhang, A. Shojaeifard, K.-K. Wong, and Z. Li, "Optimization for maximizing sum secrecy rate in SWIPT-enabled NOMA systems," *IEEE Access*, vol. 6, pp. 43440–43449, 2018.

[17] A. N. Uwaechia and N. M. Mahyuddin, "Spectrum and energy efficiency optimization for hybrid precoding-based SWIPT-enabled mmWave mMIMO-NOMA systems," *IEEE Access*, vol. 8, pp. 139994–140007, 2020.

[18] P. Nezhadmohammad, M. Abedi, M. J. Emadi, and R. Wichman, "SWIPT-enabled multiple access channel: Effects of decoding cost and non-linear EH model," *IEEE Trans. Commun.*, vol. 70, no. 1, pp. 306–316, Jan. 2022, doi: 10.1109/TCOMM.2021.3121035.

[19] N. Shanin, L. Cottatellucci, and R. Schober, "Markov decision process based design of SWIPT systems: Non-linear EH circuits, memory, and impedance mismatch," *IEEE Trans. Commun.*, vol. 69, no. 2, pp. 1259–1274, Feb. 2021.

[20] X. Xu, A. Ozcelikkale, T. McKelvey, and M. Viberg, "Simultaneous information and power transfer under a non-linear RF energy harvesting model," in *Proc. IEEE Int. Conf. Commun. Workshops (ICC Workshops)*, May 2017, pp. 179–184.

[21] M. Varasteh, B. Rassouli, and B. Clerckx, "On capacity-achieving distributions for complex AWGN channels under nonlinear power constraints and their applications to SWIPT," *IEEE Trans. Inf. Theory*, vol. 66, no. 10, pp. 6488–6508, Oct. 2020.

[22] J. H. Holland, "Outline for a logical theory of adaptive systems," *J. Assoc. Comput. Mach.*, vol. 9, no. 3, pp. 297–314, 1962, doi: 10.1145/321127.321128.

[23] M. J. Mohiz, N. K. Baloch, F. Hussain, S. Saleem, Y. B. Zikria, and H. Yu, "Application mapping using cuckoo search optimization with Lévy flight for NoC-based system," *IEEE Access*, vol. 9, pp. 141778–141789, 2021, doi: 10.1109/ACCESS.2021.3120079.

[24] J. Kennedy and R. Eberhart, "Particle swarm optimization," in *Proc. IEEE ICNN*, vol. 4, Nov./Dec. 1995, pp. 1942–1948.

[25] W.-S. Zhao, B.-X. Wang, D.-W. Wang, B. You, Q. Liu, and G. Wang, "Swarm intelligence algorithm-based optimal design of microwave microfluidic sensors," *IEEE Trans. Ind. Electron.*, vol. 69, no. 2, pp. 2077–2087, Feb. 2022.

[26] E. Valian, S. Mohanna, and S. Tavakoli, "Improved cuckoo search algorithm for feed forward neural network training," *Int. J. Artif. Intell. Appl.*, vol. 2, no. 3, pp. 36–43, Jul. 2011.

[27] I. Pavlyukevich, "Lévy flights, non-local search and simulated annealing," *J. Comput. Phys.*, vol. 226, no. 2, pp. 1830–1844, Oct. 2007.

[28] Z. Cui, B. Sun, G. Wang, Y. Xue, and J. Chen, "A novel oriented cuckoo search algorithm to improve DV-Hop performance for cyber–physical systems," *J. Parallel Distrib. Comput.*, vol. 103, pp. 42–52, May 2017.

[29] Z. Xu, Y. Yang, and B. Huang, "A teaching approach from the exhaustive search method to the needleman-wunsch algorithm," *Biochem. Mol. Biol. Educ.*, vol. 45, no. 3, pp. 194–204, Oct. 2016.

[30] T. T. Vu, H. H. Kha, T. Q. Duong, and N.-S. Vo, "Particle swarm optimization for weighted sum rate maximization in MIMO broadcast channels," *Wireless Pers. Commun.*, vol. 96, no. 3, pp. 3907–3921, May 2017.

[31] X.-S. Yang and S. Deb, "Cuckoo search via Lévy flights," in *Proc. World Congr. Nature Biol. Inspired Comput. (NaBIC)*. Coimbatore, India: IEEE, 2009.

[32] X.-S. Yang, "Nature-inspired optimization algorithms," in *Nature-Inspired Optimization Algorithms*. London, U.K.: Elsevier, 2014.

[33] R. Salgotra, U. Singh, and S. Saha, "New cuckoo search algorithms with enhanced exploration and exploitation properties," *Expert Syst. Appl.*, vol. 95, pp. 384–420, Apr. 2018.

[34] M. Grant and S. Boyd. (Jan. 2020). *CVX: MATLAB Software for Disciplined Convex Programming, Version 2.2*. [Online]. Available: http://cvxr.com/cvx

[35] X. Chen, G. Liu, Z. Ding, F. R. Yu, and P. Fan, "Power allocation for full-duplex cooperative non-orthogonal multiple access systems," in *Proc. IEEE Global Commun. Conf. (GLOBECOM)*, 2017, pp. 1–6, doi: 10.1109/GLOCOM.2017.8254641.

[36] Q. Liu, T. Lv, and Z. Lin, "Energy-efficient transmission design in cooperative relaying systems using NOMA," *IEEE Commun. Lett.*, vol. 22, no. 3, pp. 594–597, Mar. 2018.
[37] M. Wu, Q. Song, L. Guo, and A. Jamalipour, "Joint user pairing and resource allocation in a SWIPT-enabled cooperative NOMA system," *IEEE Trans. Veh. Technol.*, vol. 70, no. 7, pp. 6826–6840, Jul. 2021.
[38] Q. N. Le, A. Yadav, N.-P. Nguyen, O. A. Dobre, and R. Zhao, "Full-duplex non-orthogonal multiple access cooperative overlay spectrum-sharing networks with SWIPT," *IEEE Trans. Green Commun. Netw.*, vol. 5, no. 1, pp. 322–334, Mar. 2021.
[39] X. Li, Q. Wang, M. Liu, J. Li, H. Peng, M. J. Piran, and L. Li, "Cooperative wireless-powered NOMA relaying for B5G IoT networks with hardware impairments and channel estimation errors," *IEEE Internet Things J.*, vol. 8, no. 7, pp. 5453–5467, Apr. 2021.
[40] M. O. Okwu and L. K. Tartibu, *Metaheuristic Optimization: Nature-Inspired Algorithms Swarm and Computational Intelligence, Theory and Applications*, vol. 927. Cham, Switzerland: Springer, 2020.

CARLA E. GARCÍA (Graduate Student Member, IEEE) received the B.E. degree in electronics and telecommunications engineering from the Escuela Politécnica Nacional (EPN), Quito, Ecuador, in 2016, and the M.S. degree in electrical engineering from the University of Ulsan, South Korea, in 2020, where she is currently pursuing the Ph.D. degree with the Department of Electrical, Electronic and Computer Engineering. Her research interests include artificial intelligence, security, MIMO communications, NOMA, and optimizations.

MARIO R. CAMANA (Graduate Student Member, IEEE) received the B.E. degree in electronics and telecommunications engineering from the Escuela Politécnica Nacional (EPN), Quito, in 2016. He is currently a Graduate Research Assistant with the Department of Electrical, Electronic and Computer Engineering, University of Ulsan, Ulsan, South Korea. His research interests include machine learning, optimizations, and MIMO communications.

INSOO KOO received the B.E. degree from Konkuk University, Seoul, South Korea, in 1996, and the M.Sc. and Ph.D. degrees from the Gwangju Institute of Science and Technology (GIST), Gwangju, South Korea, in 1998 and 2002, respectively. From 2002 to 2004, he was with the Ultrafast Fiber-Optic Networks Research Center, GIST, as a Research Professor. In 2003, he was a Visiting Scholar with the Royal Institute of Science and Technology, Stockholm, Sweden. In 2005, he joined the University of Ulsan, Ulsan, South Korea, where he is currently a Full Professor. His current research interests include spectrum sensing issues for CRNs, channel and power allocation for cognitive radios (CRs) and military networks, SWIPT MIMO issues for CRs, MAC and routing protocol design for UW-ASNs, and relay selection issues in CCRNs.